Dip moveout of converted waves and parameter estimation in transversely isotropic media

Ilya Tsvankin and Vladimir Grechka

ABSTRACT

For transverse isotropy with a vertical symmetry axis (VTI media), P-wave reflection data alone are insufficient for building velocity models in *depth*. Here, we show that all parameters of VTI media responsible for $P-SV$ propagation (the P-wave and S-wave vertical velocities V_{P0} and V_{S0} and the anisotropic parameters ϵ and δ) can be obtained by combining P-wave traveltimes with the moveout of the converted PSV-wave from a horizontal and dipping reflector. Using converted modes (rather than pure S-waves) makes the method more practical by avoiding expensive shear-wave excitation.

The inversion algorithm is based on a new analytic description of the dip moveout of PS-waves developed for symmetry planes of anisotropic media (and for any vertical plane in models with *weak* azimuthal anisotropy). The common-midpoint (CMP) traveltime-offset relationship, derived in a parametric form and represented through the components of the slowness vector of the P and S-waves, makes it possible to compute the moveout curve of the PS-wave without two-point ray tracing. This formalism also yields closed-form solutions for moveout attributes, such as the coordinates ($x_{\min}$, $t_{\min}$) of the traveltime minimum and the normal-moveout (NMO) velocity defined at the apex of the moveout curve by analogy with pure modes. If reflector dip exceeds 40-50°, and CMP traveltime of the PS-wave does not have a minimum, a convenient attribute is the slope of the moveout curve (apparent slowness) at zero offset. We found a simple representation of the moveout slope in CMP geometry by proving that it is always (even in inhomogeneous media) determined by the difference between the ray parameters at the source and receiver locations.

Analytic results were incorporated into a parameter-estimation technique for VTI media (and symmetry planes of orthorhombic media), which operates with reflection moveout of P- and PS-waves from a horizontal and dipping reflector. Application of the weak-anisotropy approximation allowed us to simplify the dependence of the PS-wave moveout attributes on the anisotropic parameters and helped to design the inversion procedure. The NMO velocities of P and PS-waves from horizontal events and the ratio of the corresponding zero-offset traveltimes provide three equations for the four unknown medium parameters. The remaining parameter is found from an overdetermined system of equations that includes the P-wave NMO velocity and moveout attributes of the PS-wave for a dipping event. Numerical analysis shows that the PS-wave dip-moveout signature plays a crucial role in obtaining accurate estimates of the anisotropic parameters. The joint inversion of P and PS data provides the necessary information not only for P-wave depth imaging in VTI media, but also for the processing of PS data.

Introduction

Recent advances in the development and application of anisotropic processing algorithms (e.g., Alkhalifah et al., 1996; Anderson and Tsvankin, 1997) were made possible by new approaches to the inversion of surface seismic data for the anisotropic parameters. Alkhalifah and

Tsvankin (1995) showed that P-wave[⋆] reflection moveout and all time-processing steps [NMO and dip-moveout (DMO) corrections, prestack and poststack time migration] in VTI media depend on just two parameters – the normal-moveout velocity from a horizontal reflector $V_{\mathrm{nmo},P}(0)$ and the "anellipticity" coefficient η. In terms of Thomsen's (1986) parameters, $V_{\mathrm{nmo},P}(0)$ and η are given by

$$V_{\mathrm{nmo},P}(0) = V_{P0}\sqrt{1+2\delta}\,, \tag{1}$$

$$\eta = \frac{\epsilon-\delta}{1+2\delta}\,, \tag{2}$$

where V_{P0} is the P-wave vertical velocity, and ϵ and δ are the anisotropic parameters responsible for the velocities of P- and SV-waves. [V_{P0}, ϵ and δ are sufficient to determine all kinematic signatures of P-waves (Tsvankin, 1996), while SV-wave kinematics also depends on the shear-wave vertical velocity V_{S0}.] Both $V_{\mathrm{nmo},P}(0)$ and η can be found from surface P-wave data using either the dip dependence of NMO velocity (Alkhalifah and Tsvankin, 1995) or nonhyperbolic (long-spread) moveout of horizontal events (Alkhalifah, 1997; Grechka and Tsvankin, 1997). Grechka and Tsvankin (1996) proved that it is possible to obtain $V_{\mathrm{nmo},P}(0)$ and η from a single dipping event by performing a 3-D moveout analysis and inverting the *azimuthal* dependence of NMO velocity.

P-wave depth processing (such as prestack depth migration), however, requires knowledge of the vertical velocity V_{P0} that cannot be obtained from P-wave reflection traveltimes alone. Only if the symmetry axis of TI media is tilted by at least 30-40° from vertical, azimuthally dependent P-wave NMO velocity from two or more reflectors with different dips and/or azimuths can be inverted for all parameters which control P-wave kinematics (Grechka and Tsvankin, 1998). Thus, to resolve the vertical velocity and the anisotropic parameters of VTI media, it is necessary to supplement P-wave traveltimes with additional data. Since the SV-wave velocity also depends on the anisotropic parameters ϵ and δ, a natural option is to include reflection moveout of SV-waves into the inversion procedure. Tsvankin and Thomsen (1995) suggested combining long-spread (nonhyperbolic) moveout of P- and SV-waves from horizontal reflectors to obtain all four parameters, but this approach encounters practical problems stemming from the difficulties in acquiring and processing of long-spread shear data.

Alternatively, input data may include dip-dependent P-wave moveout (e.g., NMO velocities for two different dips), yielding the parameters $V_{\mathrm{nmo},P}(0)$ and η, and the NMO velocity of the SV-wave from a horizontal reflector:

$$V_{\mathrm{nmo},SV} = V_{S0}\sqrt{1+2\sigma}\,, \tag{3}$$

$$\sigma \equiv \left(\frac{V_{P0}}{V_{S0}}\right)^2 (\epsilon-\delta)\,. \tag{4}$$

If pure shear waves are not excited, the SV-wave NMO velocity can be determined from the NMO velocities of the P- and converted PS-waves (Seriff and Sriram, 1991):

$$t_{PS0}\,V^2_{\mathrm{nmo},PS} = t_{P0}\,V^2_{\mathrm{nmo},P} + t_{S0}\,V^2_{\mathrm{nmo},SV}\,, \tag{5}$$

where t_{P0} and t_{S0} are the vertical traveltimes of the P and S-waves, and $t_{PS0} = t_{P0} + t_{S0}$. Also, if either SV- or PSV-waves are available, the ratio of the vertical velocities can be found from the vertical traveltimes:

$$\frac{V_{P0}}{V_{S0}} = \frac{t_{S0}}{t_{P0}}\,. \tag{6}$$

In principle, equations (1), (2), (3), and (6) are sufficient to recover all four unknown parameters (V_{P0}, V_{S0}, ϵ and δ). Unfortunately, this inversion procedure turns out to be unstable, with realistic small errors in the input data propagating with considerable amplification into the inverted vertical velocities, ϵ, and δ (Grechka and Tsvankin, 1998). This instability is caused by the form of the dependence of SV-wave NMO velocity on the anisotropic parameters [equations (3) and (4)]. After obtaining $\eta \approx \epsilon - \delta$ from P-wave data and V_{P0}/V_{S0} from the vertical traveltimes, equation (3) can be used to find the S-wave vertical velocity. However, the multiplier $(V_{P0}/V_{S0})^2$ translates small errors in $\epsilon - \delta$ into substantially larger errors in σ and V_{S0}. For a typical $V_{P0}/V_{S0} = 2$, a relatively insignificant error of 0.03 in $\epsilon - \delta$ will cause a distortion of 0.12 in σ and an error of about 12% in V_{S0} and, consequently, in V_{P0}.

Here, we suggest a more stable parameter-estimation algorithm based on including dip-dependent reflection traveltimes of mode-converted PS-waves in the inversion procedure. Previous work on reflection moveout of converted waves was mostly restricted to isotropic media (e.g., Tessmer and Behle, 1988; Alfaraj, 1993). Equation (5) for NMO velocity of PSV-waves in horizontally layered VTI media was first given by Seriff and Sriram (1991). Tsvankin and Thomsen (1994) presented an analytic expression for the quartic moveout term of PSV conversions for vertical transverse isotropy and used it to describe nonhyperbolic (long-spread) reflection moveout. Anderson (1996) developed a TZO (transformation to zero offset) algorithm for vertical transverse isotropy that produces a zero-offset P-wave section from PS data.

⋆ For brevity, the qualifiers in "quasi-P-wave" and "quasi-S-wave" will be omitted.

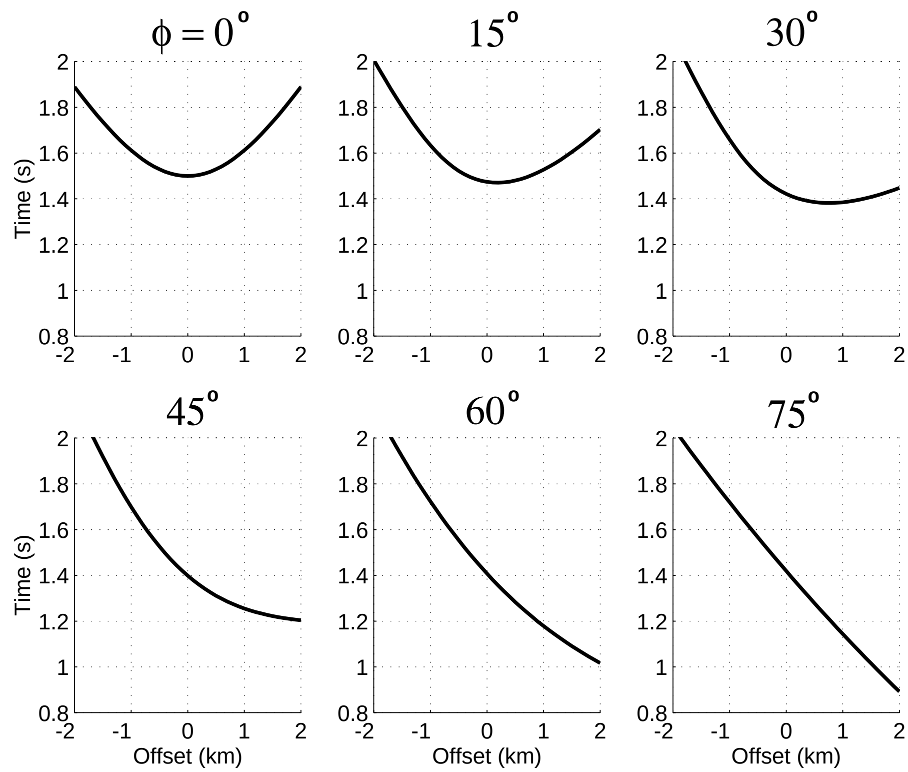

Figure 1. Dip-line reflection moveout of a PSV-wave in a homogeneous VTI layer with the parameters $V_{P0} = 2.0$ km/s, $V_{S0} = 1.0$ km/s, $\epsilon = 0.2$, $\delta = 0.1$; the distance between the CMP and the reflector is 1 km. Reflector dip is shown on top of each plot. Positive offsets correspond to the P-wave leg located downdip from the reflection point.

Reflection-point dispersal of PSV-waves in a VTI layer was discussed by Rommel (1997), who noticed a significant influence of anisotropy on the positions of sources and receivers corresponding to the same reflection point. To avoid reflection-point smear during stacking, the data should be resorted into common-reflection-point gathers, but this operation cannot be carried out without knowledge of the medium parameters. Grechka et al. (1997) showed that the azimuthal variation of NMO velocity of converted waves in horizontally layered anisotropic media with a horizontal symmetry plane always has an elliptical form [the result previously proved by Grechka and Tsvankin (1996) for pure modes]. They also generalized relationship (5) between the NMO velocities of pure and converted waves to azimuthally anisotropic media and combined NMO and vertical velocities of P and PSV-waves to obtain the parameters of a horizontal orthorhombic layer.

We begin by giving a general analytic description of reflection moveout of converted waves in a symmetry plane of a homogeneous anisotropic layer. This formalism leads to closed-form expressions for the moveout curve and its attributes (NMO velocity near the traveltime minimum, the shift of the traveltime minimum from zero offset etc.) in terms of the horizontal and vertical slowness components of the P and S-waves. For vertical transverse isotropy, we employ the weak-anisotropy approximation to simplify the exact equations and explain the relationship between the moveout attributes and medium parameters. Then we perform joint inversion of the P- and PS-wave moveout from a horizontal and dipping reflector and show that the new method yields stable estimates of the vertical velocities and anisotropic parameters of VTI media. Although the inversion algorithm is developed for vertical transverse isotropy, it remains fully valid in the vertical symmetry planes of orthorhombic media.

Dip moveout of converted waves in symmetry planes of anisotropic media

The main difference between reflection moveout of converted and pure modes in CMP geometry is that mode conversion makes the moveout curve asymmetric with respect to zero offset. Only in the special case of horizontal reflectors and a medium with a horizontal symmetry plane, converted-wave reflection traveltime is an even function of the source-receiver offset (Grechka et al., 1997). The asymmetry of the converted-wave moveout can be further enhanced by angular velocity variations in anisotropic media. Hence, in general the moveout of PS-waves cannot be described by the conventional traveltime series $t^2(x^2)$ that contains only even powers of the offset x.

Figure 1 shows typical traveltime curves of the PSV-wave computed for a common-midpoint (CMP) gather in the dip plane of a reflector beneath a VTI layer. The moveout becomes increasingly asymmetric with dip, and the traveltime minimum is recorded at "positive" offsets corresponding to the P-wave leg located *downdip* from the reflection point. For dips beyond 40°, the minimum moves to large offsets exceeding twice the CMP-reflector distance and then disappears altogether.

This behavior of PS moveout suggests using different sets of moveout attributes for mild and steep dips. If reflector dip is moderate and the PS-traveltime has a minimum on a CMP gather, it is convenient to introduce such moveout parameters, similar to those for pure modes, as the minimum traveltime $t_{\min}$, the source-receiver offset $x_{\min} = x(t_{\min})$, and the normal-moveout velocity $V_{\rm nmo}$ responsible for traveltimes near the apex (minimum) of the moveout curve. For steeper dips, a parameter that controls traveltimes at moderate source-receiver offsets is the slope of the moveout curve at $x = 0$. Below we give concise expressions for these moveout attributes and reflection traveltime as a whole for symmetry planes of an anisotropic layer.

Parametric representation of PS traveltime

Our goal here is to develop an analytic treatment of reflection moveout of converted waves in a homogeneous anisotropic layer overlying a dipping reflector. To make the problem two-dimensional, the incidence plane is assumed to coincide with both the dip plane of the reflector and a symmetry plane of the medium. [The same assumption was made by Tsvankin (1995) in his derivation of the 2-D NMO equation for pure modes.] Although our formalism is not exact outside the vertical symmetry planes, it should still provide good accuracy for models with weak azimuthal anisotropy.

In the adopted "2-D" reflection model, the phase-velocity vectors and rays of reflected waves on the dip line do not deviate from the incidence plane. Also, the polarization vector of one of the split shear modes is perpendicular to the dip (incidence) plane, and this SH-wave is completely decoupled from the P- and SV-arrivals. Therefore, a P- or SV-wave incident upon the interface generates a single converted mode (PSV or SVP); for brevity, hereafter we denote these waves simply PS and SP.

As shown in Appendix A, the traveltime and source-receiver offset of a converted wave in a CMP gather (Figure 2) can be written as

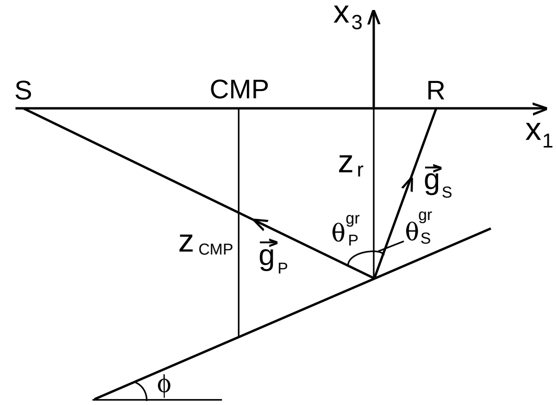

Figure 2. Reflected PS-wave in a symmetry plane of an anisotropic medium. $\vec{g}_P$ and $\vec{g}_S$ are the group-velocity vectors (rays) of the P- and S-waves, $\theta_P^{\rm gr}$ and $\theta_S^{\rm gr}$ are the corresponding group angles with vertical, $z_{\rm CMP}$ is the reflector depth beneath the CMP, and z_r is the depth of the reflection point.

$$t = z_{\rm CMP}\,\frac{N}{D} \tag{7}$$

and

$$x = z_{\rm CMP}\,\frac{N_x}{D}\,, \tag{8}$$

where $z_{\rm CMP}$ is the reflector depth beneath the common midpoint. The terms N, N_x and D depend on the reflector dip ϕ, group velocities of the P- and S-waves (g_P and g_S), and the angles between the P- and S-rays and vertical (i.e., the group angles $\theta_P^{\rm gr}$ and $\theta_S^{\rm gr}$):

$$N = \frac{1}{g_P\,\cos\theta_P^{\rm gr}} + \frac{1}{g_S\,\cos\theta_S^{\rm gr}}\,, \tag{9}$$

$$D = 1 + \frac{1}{2}\tan\phi\,(\tan\theta_P^{\rm gr} - \tan\theta_S^{\rm gr})\,, \tag{10}$$

$$N_x = \tan\theta_P^{\rm gr} + \tan\theta_S^{\rm gr}\,. \tag{11}$$

If the medium is isotropic, equations (7)–(11) become equivalent to expressions developed by Alfaraj (1993). From Snell's law it follows that the projection of the slowness vector of both P and S-waves on the interface should be identical. Hence, this slowness projection (denoted here as $p_{\rm int}$) can be conveniently used to build a parametric representation of the converted-wave reflection traveltime. For isotropic media, the angles $\theta_P^{\rm gr}$ and $\theta_S^{\rm gr}$ and reflection moveout as a whole can be obtained explicitly as functions of $p_{\rm int}$ (see Appendix A).

If the medium is anisotropic, it is necessary to solve the Christoffel equation in the Cartesian coordinate system associated with the reflector to determine the slowness vectors of the P and S-waves for a given value of $p_{\rm int}$. After rotating these vectors into the coordinate system with a vertical axis x_3 (Figure 2), equations (9)–(11) can be concisely expressed through the vertical and horizontal slowness components (Appendix A):

$$N = q_P - p_P q'_P + q_S - p_S q'_S\,, \tag{12}$$

$$D = 1 + \frac{1}{2}\tan\phi\,(q'_P + q'_S)\,, \tag{13}$$

$$N_x = q'_P - q'_S\,, \tag{14}$$

where p_P and p_S are the horizontal components of the slowness vector for the P- and S-waves (respectively), q_P and q_S are the vertical slownesses, and $q'_P \equiv dq_P/dp_P$, $q'_S \equiv dq_S/dp_S$. The x_3-axis in equations (12)–(14) is directed upward, the x_1-axis – updip, the P-wave leg is located downdip from the reflection point, and the group-velocity vectors of both waves are assumed to point towards the surface (Figure 2).

The derivative dq/dp for both waves can be obtained in a straightforward way by implicit differentiation of the Christoffel equation (Tsvankin et al., 1997). Substitution of equations (12)–(14) into equations (7) and (8) yields the offset and the corresponding traveltime of the converted wave for the CMP location with a given z_{CMP}. Although this approach involves solving the Christoffel equation for a range of slownesses p_{int}, it does not require time-consuming two-point ray tracing for each source-receiver offset.

It should be emphasized that equations (12)–(14) are valid for dip moveout of converted waves in a symmetry plane of any anisotropic medium (e.g., the model can be orthorhombic). The analytic representation of dip moveout developed in this section is used below to obtain the NMO velocity and other attributes of the moveout curve.

Attributes of the PS moveout function

The moveout attributes conventionally used in the traveltime inversion of pure-mode reflections include the normal-moveout (NMO) velocity and, sometimes, the higher-order moveout terms responsible for nonhyperbolic moveout. Due to the asymmetric shape of the common-midpoint PS moveout curve with respect to zero offset, the attribute largely responsible for small-offset reflection traveltime is the slope of the moveout curve at $x = 0$. If reflector dip is mild and the PS traveltime has a minimum at moderate offsets, suitable attributes are NMO velocity and the coordinates (offset, traveltime) of the moveout minimum.

Slope of the moveout curve and position of the traveltime minimum

In Appendix D, we show that the apparent slowness (slope) of any moveout curve recorded in CMP geometry is determined by the difference between the horizontal slownesses (ray parameters) of the incident and reflected ray measured at the source and receiver locations. This representation of moveout slope is valid in any inhomogeneous anisotropic medium if the rays in the CMP gather do not deviate from the incidence plane (i.e., the incidence plane is supposed to be a plane of mirror symmetry). The derivation in Appendix D can be easily modified for data acquired in common-shot or common-receiver gathers. The slope of reflection moveout in a shot gather, for instance, is simply equal to the ray parameter of the reflected ray at the receiver location. (This result also follows from ray theory because if the wavefield is excited by a fixed point source, the gradient of the traveltime at any point is equal to the slowness vector.)

For converted PS-waves, the slope of the $t(x)$ curve is given by

$$\frac{dt}{dx} = \frac{1}{2}\,(p_S - p_P)\,, \tag{15}$$

with the horizontal slownesses p_P and p_S measured at the source and receiver locations. Equation (15) not only provides a simple expression for the slope itself, it also helps to obtain concise solutions for NMO velocity and other attributes of the moveout minimum.

If the medium above the reflector is horizontally homogeneous (as is the case with the single-layer model considered here), both p_P and p_S remain constant between the reflector and the surface. To find the moveout slope at zero offset, we determine p_P and p_S from the condition $q'_P = q'_S$, which ensures that the group-velocity vectors of the P- and S-wave are parallel to each other.

Equation (15) can also be used to find the ray parameter $p_{\text{int}}^{\text{min}}$ corresponding to the minimum of the traveltime curve. Since the derivative dt/dx vanishes at the traveltime minimum,

$$p_P(p_{\text{int}}^{\text{min}}) = p_S(p_{\text{int}}^{\text{min}})\,. \tag{16}$$

Note that in the special case of a horizontal reflector ($\phi = 0$), equation (16) is satisfied if the slowness vectors of the incident and reflected waves are vertical ($p_P = p_S = p_{\text{int}} = 0$). Therefore, the minimum of the converted-wave traveltime from a horizontal reflector always corresponds to the vertical *slowness vector*, but the incident and reflected *rays* are not necessarily vertical, unless the medium has a horizontal symmetry plane. This means that in general the traveltime minimum of the converted wave from a horizontal reflector is located at a non-zero offset $x_{\min} \neq 0$, although the slowness vectors of the corresponding P and S-waves are vertical.

Equation (16) also confirms the well-known fact that for a pure-mode reflection and arbitrary reflector dip

$p_{\rm int}^{\rm min} = 0$. Indeed, if $p_{\rm int} = 0$, the slowness vectors of the incident and reflected waves are orthogonal to the interface and parallel to each other, so in the absence of mode conversion, $p_P = p_S$. As a result, for pure modes equation (16) is always satisfied at $p_{\rm int} = p_{\rm int}^{\rm min} = 0$, and the minimum traveltime is recorded at zero offset.

Using Snell's law and equation (16), we obtain the following relationship between the slowness components corresponding to the traveltime minimum [equation (B17)]:

$$2p_P(p_{\rm int}^{\rm min}) = [(q_P + q_S)\tan\phi]_{p_{\rm int}^{\rm min}} \,. \tag{17}$$

The vertical slownesses q_P and q_S can be found as functions of $p_P = p_S$ from the Christoffel equation. Therefore, equation (B17) can be solved in a straightforward way for the horizontal slowness $p_P(p_{\rm int}^{\rm min}) = p_S(p_{\rm int}^{\rm min})$ needed to evaluate the NMO velocity and other attributes associated with the traveltime minimum.

In Appendix B we also give an explicit solution of equation (17) for isotropic media and demonstrate that the traveltime minimum exists only if

$$\tan\phi \le \frac{2\gamma}{\gamma^2 - 1} \,, \tag{18}$$

where $\gamma \equiv V_P/V_S$, and V_P and V_S are the velocities of the P and S-waves, respectively. For a typical $\gamma = 2$, the moveout curve has a minimum for reflector dips up to 53°. Equation (18) is not exact if the medium is anisotropic, but it still provides a good approximation for small and moderate values of the anisotropic coefficients.

NMO velocity

Although the CMP traveltime of converted waves from a dipping reflector is not an even function of source-receiver offset, the moveout curve near the traveltime minimum (if it does exist) can still be described by normal-moveout velocity defined in the same way as that for pure modes:

$$V_{\rm nmo}^2 = \left\{ \frac{1}{2}\, \frac{d^2(t^2)}{dx^2} \bigg|_{x_{\rm min}} \right\}^{-1} . \tag{19}$$

Expressing both the traveltime and source-receiver offset through the slowness projection $p_{\rm int}$ and using equation (15) for the moveout slope, we obtain NMO velocity in the following form (Appendix B):

$$V_{{\rm nmo},PS}^2 = \frac{4\,(q_P''\,A_S^2 \,+\, q_S''\,A_P^2)}{(A_P + A_S)^2\,[p_P\,(q_P' + q_S') - (q_P + q_S)]} \,, \tag{20}$$

where

$$A_P = 1 + q_P' \tan\phi \,, \qquad A_S = 1 + q_S' \tan\phi \,; \tag{21}$$

the derivatives are evaluated at the slowness projection $p_{\rm int}^{\rm min}$, which is determined from equation (17).

For pure (nonconverted) modes, at the moveout minimum $q_P = q_S$, $q_P' = q_S'$, $q_P'' = q_S''$, and equation (20) reduces to the 2-D NMO equation of Tsvankin (1995) rewritten through the ray parameter (horizontal slowness) by Cohen (1998):

$$V_{\rm nmo,pure}^2 = \frac{q''}{pq' - q}\bigg|_{p_{\rm int}=0} = \frac{V(\phi)}{\cos\phi}\, \frac{\sqrt{1 + \frac{1}{V(\phi)}\frac{d^2V}{d\theta^2}\big|_{\theta=\phi}}}{1 - \frac{\tan\phi}{V(\phi)}\frac{dV}{d\theta}\big|_{\theta=\phi}} \,, \tag{22}$$

where $q' \equiv dq/dp$, and $q'' \equiv d^2q/dp^2$, and $V(\theta)$ is phase velocity as a function of phase angle with vertical. It should be mentioned that reflection-point dispersal in a CMP gather, properly treated in our approach, was not accounted for by Tsvankin (1995). The identical result of the two derivations indicates, in agreement with Hubral and Krey (1980), that reflection-point dispersal has no influence on NMO velocity for pure-mode reflections.

For a horizontal reflector ($\phi = 0$), the slowness p_P vanishes and the parameters $A_P = A_S = 1$ [equation (21)]. Hence, equation (20) becomes simply

$$V_{{\rm nmo},PS}^2(\phi = 0) = -\,\frac{q_P'' \,+\, q_S''}{q_P + q_S}\bigg|_{p_{\rm int}^{\rm min}=0} . \tag{23}$$

For media with a horizontal symmetry plane, equation (23) is fully equivalent to the VTI relationship (5). Indeed, the zero-offset ray in this case is vertical, and the ratio of the zero-offset traveltimes of the P- and S-waves is equal to the ratio of the vertical slownesses q_P and q_S:

$$\frac{t_{P0}}{t_{S0}} = \frac{q_P}{q_S} \,. \tag{24}$$

Substitution of equations (24) and (22) (for $p = 0$) into equation (23) immediately yields equation (5).

Offset of the traveltime minimum

Another potentially useful attribute of PS moveout is the offset $x_{\rm min}$ of the traveltime minimum (for pure modes, $x_{\rm min}$ always equals zero). Since $x_{\rm min}$ contains the generally unknown reflector depth $z_{\rm CMP}$, it is convenient to normalize it by the minimum traveltime $t_{\rm min}$. Using equations (7), (8), (12)–(14) and taking into account that at the traveltime minimum $p_P = p_S$ [see equation (16)], we find

$$\frac{x_{\rm min}}{t_{\rm min}} = \frac{q_P' - q_S'}{q_P + q_S - p_P(q_P' + q_S')}\bigg|_{p_{\rm int}^{\rm min}} . \tag{25}$$

By recording reflection moveout of a converted mode for a range of CMP locations in the dip plane of the reflector, we can also obtain the derivative of $t_{\rm min}$ with respect to the CMP coordinate $y_{\rm CMP} = z_{\rm CMP}/\tan\phi$. In the pure-mode case, the spatial derivative of the minimum (zero-offset) traveltime determines the slopes of reflections on the zero-offset (stacked) section and is equal to the ray parameter (horizontal slowness) of the zero-offset ray. For converted modes, $dt_{\min}/dy_{\rm CMP}$ does not have such a simple interpretation, but it can still provide useful information about the medium parameters. From equations (12)–(14) it follows that

$$\frac{dt_{\min}}{dy_{\rm CMP}} = \tan\phi\,\frac{N}{D} = \tan\phi\,\left.\frac{q_P + q_S - p_P(q'_P + q'_S)}{1 + \frac{1}{2}\tan\phi\,(q'_P + q'_S)}\right|_{p_{\rm int}^{\min}} . \qquad (26)$$

The spatial derivative $dx_{\min}/dy_{\rm CMP}$ can be expressed as a combination of $x_{\min}/t_{\min}$ [equation (25)] and $dt_{\min}/dy_{\rm CMP}$ [equation (26)] and, therefore, does not provide an independent equation for the medium parameters.

Weak-anisotropy approximation for VTI media

Analytic developments in the two previous sections are completely general and can be used in a symmetry plane of any anisotropic medium with arbitrary strength of velocity anisotropy. Here, we apply the weak-anisotropy approximation to obtain simple relationships between the moveout attributes and parameters of transversely isotropic media with a vertical symmetry axis (VTI media). These results can also be applied in the vertical symmetry planes of orthorhombic media (assuming that one of the symmetry planes is horizontal) by replacing Thomsen parameters with the equivalent notation introduced in Tsvankin (1997).

In VTI models each vertical plane is a plane of mirror symmetry, and our 2-D formalism is valid for any azimuthal orientation of the reflector. For weakly anisotropic media with small Thomsen's (1986) parameters ϵ and δ, CMP traveltime and source-receiver offset of the PS-wave can be derived as explicit functions of the projection of the slowness vector on the reflector $p_{\rm int}$ [Appendix C, equations (C11), (C13), (C14), and (C15), combined with equations (7)–(11)]. The results of Appendix C make it possible to generate reflection moveout of converted waves for weakly anisotropic VTI media without doing ray tracing and even solving the Christoffel equation.

Despite the explicit form of the weak-anisotropy approximations for traveltime and offset, they are rather lengthy and do not provide an easy insight into the influence of anisotropy on PS reflection moveout. Therefore, to simplify the expressions for NMO velocity and other attributes, we assume that not only the anisotropic coefficients, but also reflector dip is relatively small, and all terms containing the cubic and higher powers of $\sin\phi$ can be neglected.

For inversion purposes, it is convenient to replace reflector dip ϕ with the ray parameter (horizontal slowness) p_{P0} of the pure P-wave reflection recorded at zero offset (Alkhalifah and Tsvankin, 1995). Unlike reflector dip, p_{P0} can be found from surface data by measuring reflection slopes on zero-offset (stacked) P-wave sections. In the “mild-dip” approximation employed here,

$$p_{P0} \approx \frac{\sin\phi}{V_{P0}} . \qquad (27)$$

The slowness $p_{\rm int}^{\min}$ corresponding to the traveltime minimum, which for arbitrary strength of anisotropy should be obtained from equation (17), in weakly VTI media is given by (Appendix C)

$$p_{\rm int}^{\min} = \frac{\sin\phi}{2}\left(\frac{1}{V_{S0}} - \frac{1}{V_{P0}}\right) = \frac{p_{P0}}{2}\,(\gamma - 1)\,, \qquad (28)$$

where $\gamma \equiv V_{P0}/V_{S0}$. Clearly, for mild dips and in the linear approximation with respect to ϵ and δ, anisotropy has no influence on the value of $p_{\rm int}^{\min}$.

The weak-anisotropy approximation for converted-wave NMO velocity is derived in Appendix C as

$$V^{-2}_{{\rm nmo},PS}\,(p_{P0}) = V^{-2}_{{\rm nmo},PS}(0) - \frac{p^2_{P0}}{8\gamma}\left[3\gamma^4 - 2\gamma^3 + 6\gamma^2 - 2\gamma + 3\right] - \frac{p^2_{P0}\,(\gamma-1)}{2\gamma\,(\gamma+1)}\left[6\,\sigma\,(\gamma+1)^2 - (\sigma-\delta)\,\gamma\,(3\gamma^2 - 2\gamma + 3)\right] . \qquad (29)$$

The parameter σ was introduced in equation (4), and $V_{{\rm nmo},PS}(0)$ is the NMO velocity from a horizontal reflector:

$$V^{-2}_{{\rm nmo},PS}(0) = \frac{1}{V_{P0}V_{S0}}\left[1 - \frac{2(\sigma + \delta\gamma)}{1+\gamma}\right] , \qquad (30)$$

which coincides with the weak-anisotropy approximation of the exact equation (5) for $V_{{\rm nmo},PS}(0)$.

To estimate the contribution of the anisotropic parameters to the dip dependence of NMO velocity, we rewrite equations (30) and (30) for a typical velocity ratio $\gamma = 2$:

$$V^{-2}_{{\rm nmo},PS}\,(p_{P0}, \gamma = 2) = \frac{1}{V_{P0}V_{S0}}\left[1 - 1.3\,(\delta + 0.5\sigma)\right] - 3.4 p^2_{P0} - p^2_{P0}\,(2.7\sigma + 1.8\delta) . \qquad (31)$$

Thus, the anisotropic dip-dependent term $[p^2_{P0}(2.7\sigma + 1.8\delta)]$ provides an equation for σ and δ with comparable weights for both parameters. Equation (31) also shows that for positive values of σ, commonly observed in VTI formations, anisotropy amplifies the increase in the NMO velocity with dip (usually $\sigma > \delta$). However,

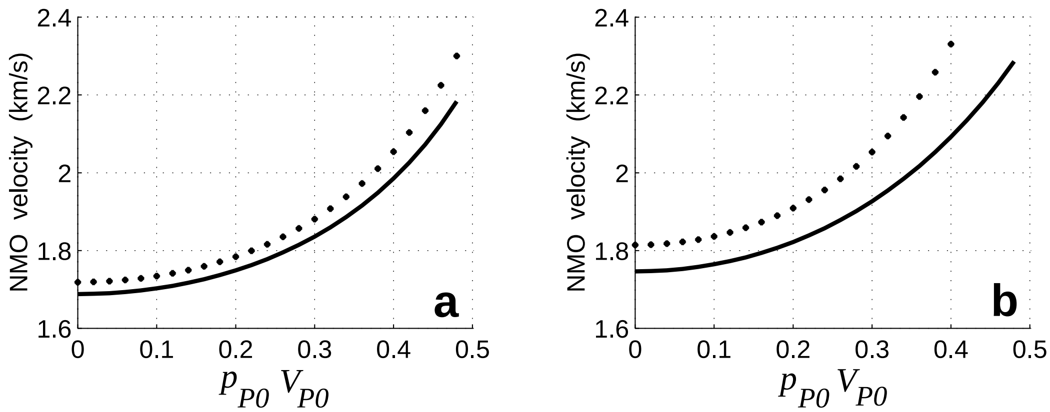

Figure 3. Exact NMO velocity of the PS-wave [equation (20), solid line] and its weak-anisotropy approximation [equation (30), dotted line] in two VTI models: (a) $\epsilon = \delta = 0.15$ (elliptical anisotropy); (b) $\epsilon = 0.15$, $\delta = 0.05$. For both media, $V_{P0} = 2.0$ km/s and $V_{S0} = 1.2$ km/s. Reflector dip changes from 0° to 30° in accordance with the P-wave ray parameter $p_{_{P0}}$ [equation (30)].

for a typical $\sigma = 0.4 - 0.5$ the magnitude of the anisotropic dip-dependent term can reach only 35-40% of the isotropic one $(3.4p_{_{P0}}^2)$, and the dip-dependence of NMO velocity as a whole is not highly sensitive to the anisotropic parameters. Our numerical tests show that the contribution of the anisotropic parameters to the exact NMO velocity is even somewhat smaller than predicted by equation (31). Therefore, we supplement the PS-wave NMO velocity in the anisotropic inversion with the normalized offset of the traveltime minimum ($x_{\min}/t_{\min}$), which proved to be more sensitive to the parameters σ and δ (see below).

The accuracy of the weak-anisotropy approximation (30) is illustrated by Figure 3. Since we retained just the leading term in ϕ and $p_{_{P0}}$, the approximation deviates from the exact solution with increasing dip. Despite this deterioration in accuracy, our approximations are sufficient for understanding the behavior of moveout attributes in the most important regime of moderate dips ($\phi < 35-40°$). For steeper dips, the traveltime minimum either does not exist at all or corresponds to unusually large source-receiver offsets seldom acquired in practice. Comparison of Figures 3a and 3b also shows that the error is higher for more "anelliptical" models with larger values of σ.

The linearized approximations for the normalized offset of the traveltime minimum ($x_{\min}/t_{\min}$) and the spatial derivative of the minimum traveltime ($dt_{\min}/dy_{\rm CMP}$) have the following form (Appendix C):

$$\frac{x_{\min}}{t_{\min}} = \frac{p_{_{P0}}\, V_{P0}^2}{2\gamma} \left[(\gamma - 1) + 2(\delta\gamma - \sigma)\right], \qquad (32)$$

$$\frac{dt_{\min}}{dy_{\rm CMP}} = p_{_{P0}}\,(1+\gamma)\,. \qquad (33)$$

The weak-anisotropy approximation (32) for $x_{\min}/t_{\min}$ is less accurate than that for NMO velocity [equation (30)] because $x_{\min}$ is already linear in $p_{_{P0}}$, and we had to drop the terms quadratic in $p_{_{P0}}$ (or in $\sin\phi$) from equation (C19) for $t_{\min}$. Still, the main value of equation (32) and other approximations in this section is in providing analytic insight into the behavior of various moveout attributes. The form of equation (32) suggests that the normalized offset $x_{\min}/t_{\min}$ is quite sensitive to the parameters δ and σ and should be included in the inversion procedure. In contrast, equation (33) for $dt_{\min}/dy_{\rm CMP}$ is purely isotropic and gives only redundant information about the ratio of the vertical velocities that can be determined in a conventional way using the vertical traveltimes [equation (6)].

The slope of the traveltime curve at zero offset in the weak-anisotropy approximation was obtained in Appendix C [equation (C28)] as

$$\left.\frac{dt}{dx}\right|_{x=0} = \frac{p_{_{P0}}}{2\,(1+\gamma)} \left[(1-\gamma^2) + 4\gamma\,(\sigma - \delta)\right]. \qquad (34)$$

For such typical values as $\gamma = 2$ and $\sigma - \delta = 0.5$, the anisotropic term in equation (34) is about 30% greater than the isotropic one. Hence, we can expect $(dt/dx)|_{x=0}$ to provide reliable information about the anisotropic parameters δ and σ (or δ and ϵ).

On the whole, analytic approximations presented above indicate that dip moveout of the converted PS-wave can be efficiently used in anisotropic parameter estimation. This conclusion is supported below by numerical inversion based on the exact equations for NMO velocity and other moveout attributes.

Parameter estimation in VTI media using dip moveout of PS-waves

As suggested by the form of the weak-anisotropy approximations, the addition of the dip moveout of PS-waves to P-wave data can help to stabilize parameter estimation in VTI media. Thus, the data used in the inversion for V_{P0}, V_{S0}, ϵ, δ include the moveout of P and PS-waves from a horizontal reflector and on the dip line of a dipping reflector. Also, we assume that the P-wave ray parameter for the dipping event (p_{P0}) was determined from the slope of the P-wave reflection on the zero-offset (stacked) section. The vertical traveltimes and NMO velocities of the P- and PS-waves from a horizontal reflector allow us to obtain the V_{P0}/V_{S0} ratio and the NMO velocity of the SV-wave [see equation (5)]. By using the P-wave NMO velocity for a dipping event [equation (22)], we include an equation for the anisotropic parameter η since $V_{\text{nmo},P}(p_{P0}) = f[V_{\text{nmo},P}(0), \eta]$. Although this information [equations (1), (2), (3), and (6)] is sufficient for determination of all four unknowns, the solution of this inverse problem, as discussed in the introduction, suffers from instability; this is further confirmed by a numerical test below. The dip-moveout attributes of the PS-wave allow us to build an overdetermined system of equations needed to obtain more accurate estimates of the vertical velocities and anisotropic parameters.

An important practical issue is how to determine the attributes associated with the PS-wave traveltime minimum ($t_{\min}$, $x_{\min}$, and $V_{\text{nmo},PS}$) from moveout data. Since the first derivative of the PS-wave traveltime curve (dt/dx) goes to zero at $x_{\min}$, we suggest to approximate the PS moveout with a hyperbola centered at the traveltime minimum:

$$t^2(x) = t^2_{\min} + \frac{(x - x_{\min})^2}{V^2_{\text{nmo},PS}}\,. \tag{35}$$

If the traveltimes have not been picked, the best-fit hyperbola can be found from semblance velocity analysis along moveout curves described by equation (35).

A typical example illustrating the application of a shifted hyperbola to the recovery of the moveout attributes is shown in Figure 4. Note that the exact PS-wave traveltimes $t(x)$ (solid) are generally asymmetric with respect to $x_{\min}$ due to the presence of a term cubic in $(x - x_{\min})$, which is not included in equation (35). This, however, does not prevent the hyperbola (35) (dashed) from giving the correct position of the moveout apex ($x_{\min}$, $t_{\min}$) and an accurate value of the NMO velocity. The errors in the estimates of V_{nmo} and $x_{\min}/t_{\min}$ [compared to the exact values given by equations (20) and (25)] are only 1.1% and 0.05%, respectively. The high accuracy achieved for the model from Figure 4 was ensured by approximately equal range of offsets on each side of the apex of the moveout curve, which mitigates the influence of the cubic moveout term. If the traveltime minimum is substantially shifted with respect to zero offset, it may be necessary either to mute out a certain range of offsets (making the fitting interval more symmetric with respect to $x_{\min}$) or add the cubic term in $x - x_{\min}$ to the moveout equation. To obtain the slope of the moveout curve at $x = 0$, we approximate the traveltimes at small source-receiver offsets with a straight line or a quadratic polynomial, depending on the moveout curvature.

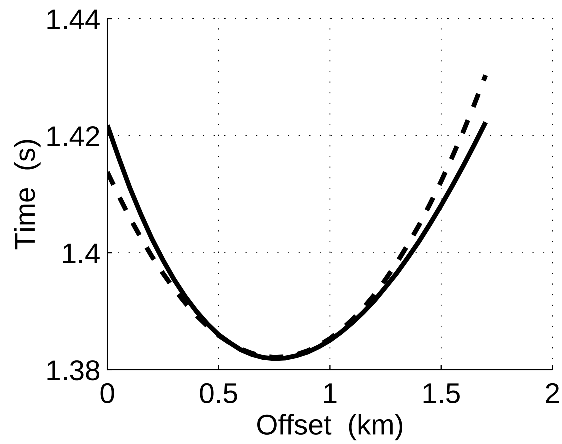

Figure 4. Exact reflection moveout of the PS-wave (solid) and its approximation with the best-fit shifted hyperbola (35) (dashed) found by least-squares minimization. The model parameters are $V_{P0} = 2.0$ km/s, $V_{S0} = 1$ km/s, $\epsilon = 0.2$, $\delta = 0.1$, $\phi = 30°$.

Our inversion algorithm is organized in the following way. Using the relationship between the NMO velocities for horizontal events [equation (5)], we determine the SV-wave NMO velocity [equation (3)] from P and PS data. Then, for a given value of δ, we find the other three parameters [see equations (1), (3), (4), (6)]:

$$V_{P0} = \frac{V_{\text{nmo},P}}{\sqrt{1+2\delta}}\,, \tag{36}$$

$$V_{S0} = \frac{V_{P0}}{\gamma}\,, \tag{37}$$

$$\sigma = \frac{1}{2}\left[\frac{V^2_{\text{nmo},SV}}{V^2_{S0}} - 1\right]\,, \tag{38}$$

$$\epsilon = \frac{\sigma}{\gamma^2} + \delta\,. \tag{39}$$

The last step is to use the P-wave NMO velocity $V_{\text{nmo},P}(p_{P0})$ and PS-wave moveout attributes for the

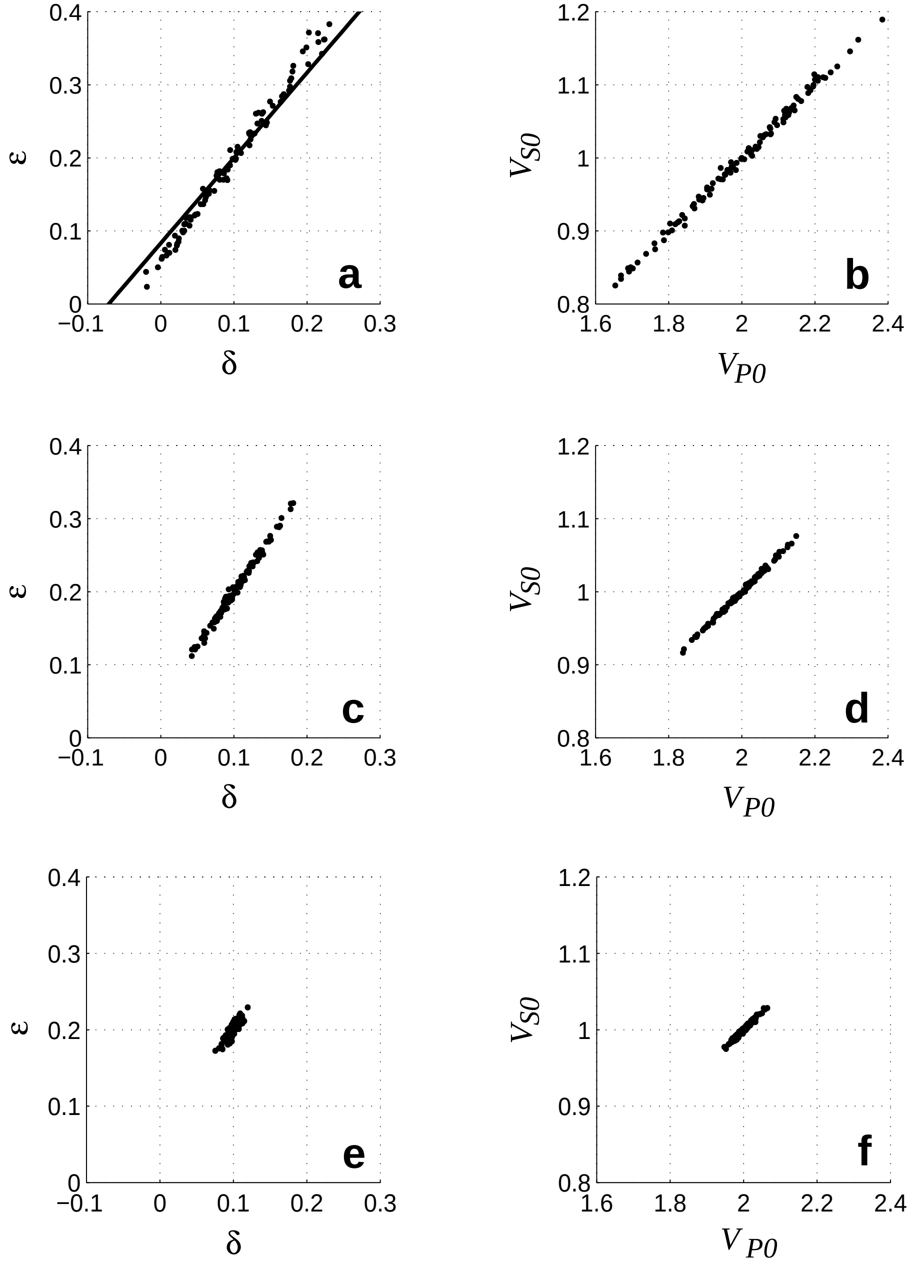

Figure 5. Parameters ϵ, δ, V_{P0}, and V_{S0} determined by inverting P and PS moveout data from a horizontal and dipping reflector. The input data were distorted by random noise with a variance of 0.5% for γ, 1.5% for the zero-dip NMO velocities and 2% for the moveout attributes of the dipping event. (a) and (b) Inversion *without* dip-moveout attributes of the PS-wave; the dip $\phi = 30°$. (c) and (d) Inversion including the dip-moveout attributes of the traveltime minimum of the PS-wave [equation (40)]; the dip $\phi = 30°$. (e) and (f) Inversion including the slope of the PS-moveout curve [equation (41)]; the dip $\phi = 50°$. The actual values are: $V_{P0} = 2.0$ km/s, $V_{S0} = 1$ km/s, $\epsilon = 0.2$, $\delta = 0.1$. The solid line on plot (a) indicates ϵ's and δ's corresponding to the correct value of η ($\eta = 0.083$).

same dipping reflector to invert for the remaining unknown parameter δ. If the PS traveltime does have a minimum on the CMP gather, δ is found by minimizing an objective function that contains the PS moveout attributes $V_{\text{nmo},PS}(p_{P0})$ and $x_{\min}/t_{\min}$:

$$\mathcal{F}^{(1)}_{P,SV} = \left[\frac{V_{\text{nmo},P}(p_{P0}) - V^{\text{meas}}_{\text{nmo},P}(p_{P0})}{V^{\text{meas}}_{\text{nmo},P}(p_{P0})}\right]^2 + \left[\frac{V_{\text{nmo},PS}(p_{P0}) - V^{\text{meas}}_{\text{nmo},PS}(p_{P0})}{V^{\text{meas}}_{\text{nmo},PS}(p_{P0})}\right]^2 + \left[\frac{(x_{\min}/t_{\min}) - (x_{\min}/t_{\min})^{\text{meas}}}{(x_{\min}/t_{\min})^{\text{meas}}}\right]^2 . \qquad (40)$$

Here the superscript "meas" denotes the values measured from the data, while the quantities without the subscript are computed from the exact equations (20), (22) and (25). Essentially, the objective function (40) represents an overdetermined system of three nonlinear equations for the single unknown parameter δ.

For PS traveltime curves without a minimum, the objective function contains a different PS moveout attribute – the slope of the moveout curve at $x = 0$ [equation (15)]:

$$\mathcal{F}^{(2)}_{P,SV} = \left[\frac{V_{\text{nmo},P}(p_{P0}) - V^{\text{meas}}_{\text{nmo},P}(p_{P0})}{V^{\text{meas}}_{\text{nmo},P}(p_{P0})}\right]^2 + \left[\frac{(dt/dx|_{x=0}) - (dt/dx|_{x=0})^{\text{meas}}}{(dt/dx|_{x=0})^{\text{meas}}}\right]^2 . \qquad (41)$$

In principle, $(dt/dx|_{x=0})$ can be used in the inversion for mild dips as well. However, if the traveltime minimum is close to zero offset, the slope of the moveout curve at $x = 0$ is accurately described by the best-fit shifted hyperbola and, therefore, becomes a redundant attribute.

A numerical example of the joint inversion of P and PS data based on equations (36)–(41) is displayed in Figure 5. All input parameters were computed from the exact equations and distorted by Gaussian noise with variances simulating realistic errors in data measurements. To generate the top row of plots (Figures 5a,b), we removed the terms involving the moveout attributes of the PS-wave from the objective function (40). As expected, the parameter η can be accurately determined from the P-wave NMO velocity of the dipping event, and the ϵ and δ points in Figure 5a are close to the line corresponding to the correct value of η. However, the inversion results for V_{P0}, V_{S0}, ϵ, and δ exhibit significant scatter indicative of high sensitivity to errors in the input data. The standard deviations in all four parameters are too significant for this algorithm to be used in practice (8.6% for V_{P0} and V_{S0}, 0.13 for ϵ and 0.09 for δ).

Minimization using the full objective function (40) (including the NMO velocity of the PS-wave and the normalized offset $x_{\min}/t_{\min}$) leads to a dramatic reduction in the scatter for all medium parameters, with standard deviations of only 3.4% for V_{P0} and V_{S0}, 0.05 for ϵ and 0.03 for δ (Figures 5c,d). Clearly, the dip-moveout attributes of the PS-wave allowed us to overcome the problem of error amplification in the transition from η to the vertical velocities and anisotropic coefficients.

Figures 5a-d correspond to a relatively mild reflector dip of 30°. As the dip reaches 50°, the CMP traveltime of the PS-wave no longer has a minimum, and we need to use the second form of the objective function [equation (41)] that includes the slope of the PS moveout curve at zero offset (Figures 5e,f). Since the moveout attributes of both P and PS-waves become more sensitive to the anisotropic parameters with increasing dip, the inversion results for the $\phi = 50°$ are even better than those for $\phi = 30°$ (the standard deviations are 1.2% for V_{P0} and V_{S0}, and 0.01 for ϵ and δ).

Discussion and conclusions

Determination of the vertical velocity and the anisotropic parameters of VTI media from surface data is impossible without combining reflection moveout of P-waves with S-wave traveltimes. Since shear waves are seldom excited in exploration surveys, a more practical option is to supplement P-wave moveout with converted-wave data. Analysis of the kinematic inverse problem shows that it is necessary to include PS (PSV) traveltimes not just from a horizontal reflector, but also from at least one dipping interface.

Moveout of PS-waves generally is asymmetric with respect to zero offset, with the position of the traveltime minimum strongly dependent on reflector dip. For relatively mild dips up to 30-40°, the minimum usually corresponds to moderate offsets and can be recorded in a conventional-length CMP gather. In this case, PS traveltimes can be used to recover moveout attributes associated with the traveltime minimum $t_{\min}(x_{\min})$, such as the normal-moveout velocity (defined by analogy with pure modes) and the ratio $x_{\min}/t_{\min}$. We show that these attributes can be obtained from reflection data by approximating PS-moveout with a *shifted* hyperbola centered at the offset $x_{\min}$. If reflector dip exceeds $40 - 50°$, the traveltime minimum either does not exist at all or cannot be captured on conventional spreads. For these traveltime functions, monotonically decreasing with offset, a natural attribute is the slope of the moveout curve at the CMP location.

To apply the PS-wave moveout attributes in anisotropic parameter estimation, we developed an analytic treatment of dip moveout of converted waves valid in a vertical symmetry plane of an anisotropic layer with arbitrary strength of anisotropy (e.g., the model can be orthorhombic). Parametric representation of the PS traveltime and CMP offset in terms of the slowness projection on the reflector yields a concise description for reflection moveout involving the vertical and horizontal slowness components of the P- and S-waves. Although the computation of the source-receiver offset and corresponding traveltime involves solving the Christoffel equation in the coordinate system associated with the reflector, our expression can be used to generate the CMP moveout curve without time-consuming two-point ray tracing.

We also proved that the slope of any moveout curve in CMP geometry is always equal to one half of the difference between the ray parameters (horizontal slownesses) evaluated for the incident and reflected ray at the source and receiver locations. This simple result is valid not just for a single layer, but for arbitrary inhomogeneous anisotropic media provided the rays do not deviate from the incidence plane. Combined with the parametric traveltime-offset relationships, the description of moveout slope in terms of the horizontal slownesses of the P and S-waves made it possible to derive closed-form expressions for all moveout attributes described above.

These analytic developments provide a basis for a joint inversion of P and PS data in VTI media. The weak-anisotropy approximation allowed us to find explicit expressions for the traveltime and offset of the PS-wave and study the dependence of the moveout attributes on the anisotropic parameters. The attributes proved to be mostly sensitive to the anisotropy are the normalized offset $x_{\min}/t_{\min}$ and the slope of the $t(x)$ curve at zero offset, while the contribution of anisotropy to the dip-dependence of the PS-wave NMO velocity is noticeably smaller.

Our inversion algorithm is designed to recover the medium parameters (the P- and S-wave vertical velocities V_{P0} and V_{S0} and the anisotropic coefficients ϵ and δ) using the NMO velocities and vertical traveltimes of the P and PS-waves from a horizontal reflector, P-wave NMO velocity from a dipping reflector, and PS moveout attributes for the same dipping event. Although the number of equations is sufficient to obtain all unknowns even without the dip-moveout attributes of the PS-wave, such an inversion procedure is rather unstable. While the parameter $\eta \approx \epsilon - \delta$ is well-constrained by the dip dependence of P-wave moveout, small errors in η propagate with considerable amplification into the vertical velocities and anisotropic parameters. The addition of the PS moveout attributes to the input data leads to a dramatic improvement in the stability of the inversion procedure. It is interesting that the disappearance of the PS traveltime minimum at steep dips does not impair the stability of the parameter estimation. On the contrary, the accuracy in all inverted parameters increases with dip due to the higher sensitivity of the dip-moveout attributes to the anisotropy.

We showed that combining P and PS reflection traveltimes in moveout inversion yields all parameters of VTI media needed for *depth* imaging of P, SV, or PSV-waves. Therefore, one of the most important applications of our method is in building velocity models for P-wave prestack or poststack depth migration. Processing of converted waves in VTI media is also impossible without knowledge of both vertical velocities and the parameters ϵ and δ. Although our inversion has to be performed on common-midpoint gathers, reflection-point dispersal makes it necessary to resort the data into common-reflection-point (CRP) gathers prior to stacking. This operation was proved to be sensitive to the anisotropic coefficients of VTI media and vertical velocities (Rommel, 1997). An alternative way to generate a zero-offset section for converted waves is the transformation to zero offset (TZO), which also requires an accurate VTI model (Anderson, 1996). In addition, our analytic expressions for the converted-wave reflection moveout can be used to extend dip-moveout processing algorithms to PS-modes in anisotropic media.

Due to the kinematic equivalence between the symmetry planes of orthorhombic and VTI media, our results remain valid for CMP reflections in both vertical symmetry planes of models with orthorhombic symmetry (Tsvankin, 1997). The only change required in the weak-anisotropy approximations and the inversion algorithm as a whole is the replacement of ϵ, δ, and the shear-wave vertical velocity V_{S0} with the appropriate set of parameters introduced by Tsvankin (1997).

It is likely that the accuracy of the moveout inversion can be further increased by treating azimuthally varying PS traveltimes in addition to the moveout in the dip plane of the reflector. This methodology can be based on the extension of the 3-D NMO equation, which was originally developed by Grechka and Tsvankin (1996) for pure modes and later generalized by Grechka et al. (1997) for converted waves in horizontally layered media. In sequel publications, we will also discuss the inversion of the PS-moveout attributes for layered anisotropic media.

Acknowledgments

We are grateful to members of the A(nisotropy)-Team of the Center for Wave Phenomena (CWP) at CSM for helpful discussions.

References

Alfaraj, M.N., 1993, Transformation to zero offset for mode-converted waves: Ph.D. thesis, Colorado School of Mines.

Alkhalifah, T., 1997, Velocity analysis using nonhyperbolic moveout in transversely isotropic media: Geophysics, **62**, 1839–1855.

Alkhalifah, T., Tsvankin, I., Larner, K., and Toldi, J., 1996, Velocity analysis and imaging in transversely isotropic media: Methodology and a case study: The Leading Edge, **15**, no. 5, 371–378.

Alkhalifah, T., and Tsvankin, I., 1995, Velocity analysis in transversely isotropic media: Geophysics, **60**, 1550–1566.

Anderson, J.E., 1996, Imaging in transversely isotropic media with a vertical symmetry axis, Ph.D. thesis, Colorado School of Mines.

Anderson, J.E., and Tsvankin, I., 1997, Dip-moveout processing by Fourier transform in anisotropic media: Geophysics, **62**, 1260–1269.

Cohen, J.K., 1998, A convenient expression for the NMO velocity function in terms of ray parameter: Geophysics, **63**, 275–278.

Grechka, V., Theophanis, S., and Tsvankin, I., 1997, Joint inversion of P- and PS-waves in orthorhombic media: Theory and a physical-modeling study: 67th Ann. Internat. Mtg., Soc. Expl. Geophys., Expanded Abstracts, 1250–1253 (also CWP-245).

Grechka, V., and Tsvankin, I., 1996, 3-D description of normal moveout in anisotropic media: 66th Ann. Internat. Mtg., Soc. Expl. Geophys., Expanded Abstracts, 1487–1490 (also Geophysics, May 1998).

Grechka, V., and Tsvankin, I., 1997, Feasibility of nonhyperbolic moveout inversion in transversely isotropic media: submitted to Geophysics.

Grechka, V., and Tsvankin, I., 1998, Inversion of azimuthally dependent NMO velocity in transversely isotropic media with a tilted axis of symmetry: CWP Research Report, this volume.

Hubral, P., and Krey, T., 1980, Interval velocities from seismic reflection measurements: Soc. Expl. Geophys.

Rommel, B., 1997, Stacking charts for converted waves in a transversely isotropic medium: CWP Project Review (CWP-252).

Seriff, A.J., and Sriram, K.P., 1991, P-SV reflection moveouts for transversely isotropic media with a vertical symmetry axis: Geophysics, **56**, 1271–1274.

Tessmer, G., and Behle, A., 1988, Common reflection point data-stacking technique for converted waves: Geophys. Prosp., **36**, 671–688.

Thomsen, L., 1986, Weak elastic anisotropy: Geophysics, **51**, 1954–1966.

Tsvankin, I., 1995, Normal moveout from dipping reflectors in anisotropic media: Geophysics, **60**, 268–284.

Tsvankin, I., 1996, P-wave signatures and notation for transversely isotropic media: An overview: Geophysics, **61**, 467–483.

Tsvankin, I., 1997, Anisotropic parameters and P-wave velocity for orthorhombic media: Geophysics, **62**, 1292–1309.

Tsvankin, I., and Thomsen, L., 1994, Nonhyperbolic reflection moveout in anisotropic media: Geophysics, **59**, 1290–1304.

Tsvankin, I., and Thomsen, L., 1995, Inversion of reflection traveltimes for transverse isotropy: Geophysics, **60**, 1075–1107.

Tsvankin, I., Grechka, V., and Cohen, J.K., 1997, Generalized Dix equation and modeling of normal moveout in inhomogeneous anisotropic media: 67th Ann. Internat. Mtg., Soc. Expl. Geophys., Expanded Abstracts, 1246–1249.

APPENDIX A: Converted-wave moveout from dipping reflectors

Let us consider a PS-wave recorded in CMP geometry in the dip direction of a plane reflector. It is assumed that the incidence plane also represents a symmetry plane of the medium, so both rays and the corresponding phase-velocity vectors of the reflected waves are confined to the incidence plane; also, the P-wave generates only one (PSV) conversion. Without losing generality, we assume that the P-leg is located downdip from the reflection point (Figure 2). Then the reflection traveltime can be written as

$$t = t_P + t_S = \frac{z_r}{g_P \cos\theta_P^{\rm gr}} + \frac{z_r}{g_S \cos\theta_S^{\rm gr}}\,, \tag{A1}$$

where $\theta_P^{\rm gr}$ and $\theta_S^{\rm gr}$ are the group angles with vertical for the P and S segments of the reflected ray (Figure 2), g_P and g_S are the corresponding group velocities, and z_r is the depth of the reflection point. The source-receiver offset in terms of the group angles is given by

$$x = x_P + x_S = z_r\,(\tan\theta_P^{\rm gr} + \tan\theta_S^{\rm gr})\,. \tag{A2}$$

The angle $\theta_S^{\rm gr}$ in equation (A1) and below is considered negative if the S-ray is tilted toward the CMP from the reflection point. Introducing the reflector depth beneath the common midpoint ($z_{\rm CMP}$) instead of z_r yields

$$z_{\rm CMP} = z_r\,[1 + \frac{1}{2}\tan\phi\,(\tan\theta_P^{\rm gr} - \tan\theta_S^{\rm gr})]\,, \tag{A3}$$

ϕ is reflector dip. Substituting $z_{\rm CMP}$ [equation (A3)] into equations (A1) and (A2), we find

$$t = z_{\rm CMP}\,\frac{N}{D} \tag{A4}$$

and

$$x = z_{\rm CMP}\,\frac{N_x}{D}\,, \tag{A5}$$

where

$$N = \frac{1}{g_P\,\cos\theta_P^{\rm gr}} + \frac{1}{g_S\,\cos\theta_S^{\rm gr}}\,, \tag{A6}$$

$$D = 1 + \frac{1}{2}\tan\phi\,(\tan\theta_P^{\rm gr} - \tan\theta_S^{\rm gr})\,, \tag{A7}$$

$$N_x = \tan\theta_P^{\rm gr} + \tan\theta_S^{\rm gr}\,. \tag{A8}$$

To satisfy Snell's law, the P and S-waves should have the same projection of the slowness vector (ray parameter) on the interface at the reflection point. Hence, this projection ($p_{\rm int}$; the subscript stands for the interface) can be conveniently used to build a parametric representation of the converted-wave CMP traveltime. Hereafter, we assume that $p_{\rm int}$ is the "updip" projection that corresponds to the upgoing S-wave and downgoing P-wave.

If the medium is isotropic, the group angles $\theta_P^{\rm gr}$ and $\theta_S^{\rm gr}$ are equal to the corresponding phase angles and can be easily expressed through $p_{\rm int}$ (taken to be non-negative), reflector dip ϕ, and the velocities of the P- and S-waves (V_P and V_S):

$$\sin\theta_P^{\rm gr} = p_{\rm int}V_P\cos\phi + \sqrt{1-p_{\rm int}^2V_P^2}\,\sin\phi\,, \tag{A9}$$

$$\cos\theta_P^{\rm gr} = \sqrt{1-p_{\rm int}^2V_P^2}\,\cos\phi - p_{\rm int}V_P\sin\phi\,, \tag{A10}$$

$$\sin\theta_S^{\rm gr} = p_{\rm int}V_S\cos\phi - \sqrt{1-p_{\rm int}^2V_S^2}\,\sin\phi\,, \tag{A11}$$

$$\cos\theta_S^{\rm gr} = \sqrt{1-p_{\rm int}^2V_S^2}\,\cos\phi + p_{\rm int}V_S\sin\phi\,. \tag{A12}$$

Substitution of equations (A9)–(A12) into equations (A6)–(A8) and then (A4) and (A5) leads to explicit expressions for the reflection traveltime and source-receiver offset in CMP geometry in terms of the slowness $p_{\rm int}$.

For anisotropic media, the transition from the slowness (ray parameter) $p_{\rm int}$ to the group angles of the reflected waves involves solving the Christoffel equation for the slowness component orthogonal to the reflector. For $P-SV$-waves in a symmetry plane of an anisotropic medium, the Christoffel equation for an unknown slowness component is quartic (it becomes sextic outside the symmetry planes).

Since we may have several reflectors with different dips in the same medium, it is more convenient to express the traveltime curve through the slowness components in the unrotated coordinate system associated with the earth surface. Also, note that the group angles in equations (A1)–(A5) are defined with respect to the vertical axis rather than the reflector normal. Introducing the projections of the group-velocity vectors of P- and S-waves on the vertical (x_3, subscript "3") and horizontal (x_1, subscript "1") axes, we obtain the following equivalent form of equations (A6)–(A8):

$$N = \frac{1}{g_{P3}} + \frac{1}{g_{S3}}\,, \tag{A13}$$

$$D = 1 - \frac{1}{2}\tan\phi\,(\frac{g_{P1}}{g_{P3}} + \frac{g_{S1}}{g_{S3}})\,, \tag{A14}$$

$$N_x = -\frac{g_{P1}}{g_{P3}} + \frac{g_{S1}}{g_{S3}}\,. \tag{A15}$$

Here the x_3-axis is directed upward, the x_1-axis – updip, and both group-velocity vectors are assumed to point from the reflector towards the surface. The group-velocity components can be related to the slowness vector in the same (unrotated) coordinate system in the following way (Tsvankin et al., 1997):

$$g_3 = \frac{1}{q - pq'} \tag{A16}$$

and

$$g_1 = -g_3 q'\,, \tag{A17}$$

where q and p are the vertical and horizontal slowness components, respectively, and $q' \equiv dq/dp$. Equations (A16) and (A17) allow us to rewrite equations (A13)–(A15) as

$$N = q_P - p_P q_P' + q_S - p_S q_S'\,, \tag{A18}$$

$$D = 1 + \frac{1}{2}\tan\phi\,(q'_P + q'_S)\,, \tag{A19}$$

$$N_x = q'_P - q'_S\,. \tag{A20}$$

Here p_P and p_S are the horizontal components of the slowness vector for the P- and S-waves, and $q'_P \equiv dq_P/dp_P$, $q'_S \equiv dq_S/dp_S$.

To generate a CMP gather of the converted PS-wave, we first need to obtain p_P and p_S as functions of the projection of the slowness vector on the reflector ($p_{\rm int}$) by solving the Christoffel equation for the slowness vectors of the P- and S-waves in the rotated coordinate system with one of the axes parallel to the reflecting interface. Then we can find p_P and p_S and use them in equations (A18)–(A20), (A4), and (A5) to obtain the moveout curve of the converted mode.

APPENDIX B: NMO velocity for converted-wave moveout

If reflection moveout of a converted wave in a CMP gather does have a minimum $t_{\rm min} = t(x_{\rm min})$, the traveltime near $t_{\rm min}$ can be described by normal-moveout velocity $V_{\rm nmo}$ introduced by analogy with pure modes. To find an analytic expression for $V_{\rm nmo}$, we expand the squared CMP traveltime $t^2(x)$ into a Taylor series near the traveltime minimum:

$$t^2(x) = t^2_{\rm min} + \left.\frac{d(t^2)}{dx}\right|_{x_{\rm min}} (x - x_{\rm min}) + \frac{1}{2}\left.\frac{d^2(t^2)}{dx^2}\right|_{x_{\rm min}} (x - x_{\rm min})^2 + \dots \tag{B1}$$

The first derivative $d(t^2)/dx$ at $x = x_{\rm min}$ is equal to zero, while the second derivative yields the NMO velocity that governs the traveltime for small $(x - x_{\rm min})$:

$$V^2_{\rm nmo} = \left\{\frac{1}{2}\left.\frac{d^2(t^2)}{dx^2}\right|_{x_{\rm min}}\right\}^{-1} = \left\{t\,\frac{d}{dx}\left(\frac{dt}{dx}\right)\Big|_{x_{\rm min}}\right\}^{-1}. \tag{B2}$$

Using the results of Appendix D, the moveout slope dt/dx can be expressed through the difference between the horizontal slownesses of the P- and S-waves:

$$\frac{dt}{dx} = \frac{1}{2}\,(p_S - p_P)\,. \tag{B3}$$

Considering both dt/dx and x as functions of the projection of the slowness vector on the interface ($p_{\rm int}$), we can rewrite equation (B2) as

$$V^2_{{\rm nmo},PS} = \left\{\frac{t}{2}\left.\frac{d(p_S - p_P)/dp_{\rm int}}{dx/dp_{\rm int}}\right|_{p^{\rm min}_{\rm int}}\right\}^{-1}, \tag{B4}$$

where $p^{\rm min}_{\rm int}$ corresponds to the traveltime minimum.

To evaluate the derivatives in equation (B4), $p_{\rm int}$ should be represented through the slownesses of the P- and S-waves using Snell's law:

$$p_{\rm int} = -(p_P\cos\phi + q_P\sin\phi) = p_S\cos\phi + q_S\sin\phi\,. \tag{B5}$$

The P-wave in equations (A13)–(A15) is assumed to travel *upward* from the reflector, which explains the minus sign in front of the P-wave term in equation (B5). Differentiating equation (B5), we obtain

$$\frac{dp_P}{dp_{\rm int}} = -(\cos\phi + q'_P\sin\phi)^{-1}\,, \tag{B6}$$

$$\frac{dp_S}{dp_{\rm int}} = (\cos\phi + q'_S\sin\phi)^{-1}\,, \tag{B7}$$

where, as in equations (A18)–(A20), $q'_P \equiv dq_P/dp_P$ and $q'_S \equiv dq_S/dp_S$. Hence,

$$\frac{d(p_S - p_P)}{dp_{\rm int}} = \frac{1}{\cos\phi}\left[\frac{1}{1 + q'_P\tan\phi} + \frac{1}{1 + q'_S\tan\phi}\right]. \tag{B8}$$

The derivative $dx/dp_{\rm int}$ in equation (B4) can be represented through D and N_x [equations (A19) and (A20)] as

$$\frac{dx}{dp_{\rm int}} = z_{\rm CMP}\,\frac{d(N_x/D)}{dp_{\rm int}} = z_{\rm CMP}\,\frac{(dN_x/dp_{\rm int})\,D - (dD/dp_{\rm int})\,N_x}{D^2}\,. \tag{B9}$$

Equations (B6) and (B7) allow us to express the derivatives with respect to $p_{\rm int}$ through those with respect to p_P or p_S; for instance,

$$\frac{dq_P}{dp_{\rm int}} = -q'_P(\cos\phi + q'_P \sin\phi)^{-1}\,. \tag{B10}$$

Equation (B10) and an analogous expression for q_S allow us to obtain the numerator in equation (B9) in the following form:

$$\frac{dN_x}{dp_{\rm int}}D - \frac{dD}{dp_{\rm int}}N_x = -\frac{q''_P\,(1+q'_S\,\tan\phi)}{\cos\phi + q'_P\sin\phi} - \frac{q''_S\,(1+q'_P\,\tan\phi)}{\cos\phi + q'_S\sin\phi}\,. \tag{B11}$$

Note the symmetry in equation (B11) with respect to the subscripts "P" and "S": the second term can be obtained by interchanging these subscripts in the first term. The expression for D, also needed in equation (B9), was derived previously [equation (A19)]:

$$D = 1 + \frac{1}{2}\tan\phi\,(q'_P + q'_S)\,. \tag{B12}$$

Equations (B11) and (B12) are sufficient for obtaining the derivative $dx/dp_{\rm int}$ from equation (B9).

NMO velocity, as given by equation (B4), also depends on the minimum traveltime that can be found from equations (A4), (A18), and (A19):

$$t_{\rm min} = t(p^{\rm min}_{\rm int}) = z_{\rm CMP}\left.\frac{q_P - p_P q'_P + q_S - p_S q'_S}{1+\frac{1}{2}\tan\phi\,(q'_P + q'_S)}\right|_{p^{\rm min}_{\rm int}}\,. \tag{B13}$$

Substituting equations (B8), (B9) and (B13) into equation (B4) and taking into account that at the traveltime minimum $p_P = p_S$ [see equation (B16) below] yields the final expression for NMO velocity as a function of the horizontal slownesses of the P- and S-waves:

$$V^2_{{\rm nmo},PS} = \left.\frac{4\,(q''_P\,A^2_S\, + q''_S\,A^2_P)}{(A_P + A_S)^2\,[p_P\,(q'_P + q'_S) - (q_P + q_S)]}\right|_{p^{\rm min}_{\rm int}}\,, \tag{B14}$$

where

$$A_P = 1 + q'_P\tan\phi\,, \qquad A_S = 1 + q'_S\tan\phi\,. \tag{B15}$$

To obtain the ray parameter $p^{\rm min}_{\rm int}$, we use equation (B3) for the slope of the moveout curve. Since at the traveltime minimum the slope goes to zero,

$$p_P(p^{\rm min}_{\rm int}) = p_S(p^{\rm min}_{\rm int})\,. \tag{B16}$$

Substituting $p_P = p_S$ into Snell's law [equation (B5)] and dividing both sides by $\cos\phi$ gives the following equation for the slownesses corresponding to the traveltime minimum:

$$2p_P(p^{\rm min}_{\rm int}) = [(q_P + q_S)\tan\phi]_{p^{\rm min}_{\rm int}}\,. \tag{B17}$$

where the vertical slownesses q_P and q_S are related to $p_P = p_S$ through the Christoffel equation.

For isotropic media, the vertical slownesses are given simply by

$$q_P = \sqrt{\frac{1}{V^2_P} - p^2_P} \tag{B18}$$

and

$$q_S = \sqrt{\frac{1}{V^2_S} - p^2_S}\,. \tag{B19}$$

In this case, it is possible to derive an explicit expression for $p_P(p^{\rm min}_{\rm int}) = p_S(p^{\rm min}_{\rm int})$ by solving equation (B17) with q_P and q_S from equations (B18) and (B19):

$$p_P(p^{\rm min}_{\rm int}) = \frac{\sin\phi}{2\,V_P}\sqrt{1+\gamma^2+S}\,, \tag{B20}$$

where $\gamma \equiv V_P/V_S$ and

$$S = \sqrt{4\gamma^2 - \tan^2\phi\,(\gamma^2-1)^2}\,. \tag{B21}$$

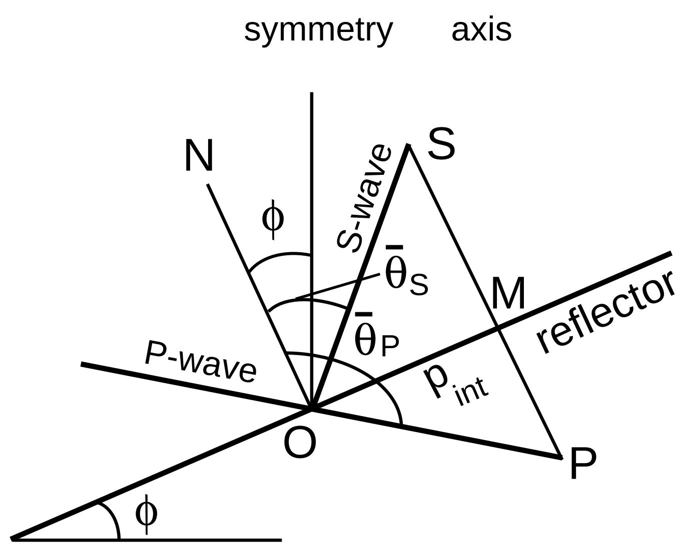

Figure C1. To the derivation of the weak-anisotropy approximation for PS moveout. OP and OS are the slowness (phase-velocity) directions of the downgoing P- and upgoing S-legs of the converted wave, and $\bar{\theta}_P$ and $\bar{\theta}_S$ are the corresponding phase (slowness) angles with the reflector normal ON. OM is the projection of the slowness vectors on the reflector (denoted as p_{int}) that should be identical for the P- and S-waves.

This solution, however, exists only if the expression under the radical in equation (B21) is nonnegative, or

$$\tan\phi \le \frac{2\gamma}{\gamma^2 - 1}\,. \tag{B22}$$

APPENDIX C: Weak-anisotropy approximation for converted-wave moveout in VTI media

Here we derive weak-anisotropy approximations for the traveltime-offset relationship and moveout attributes of PS-waves in VTI media by carrying out linearization in Thomsen's parameters ϵ and δ. For small $|\epsilon| \ll 1$ and $|\delta| \ll 1$, phase velocities of P- and $S(SV)$-waves can be well-approximated by the following linearized expressions (Thomsen, 1986):

$$V_P(\hat{\theta}) = V_{P0}\,[1 + \delta \sin^2\hat{\theta} + (\epsilon - \delta)\sin^4\hat{\theta}] \tag{C1}$$

and

$$V_{SV}(\hat{\theta}) = V_{S0}\,(1 + \sigma \sin^2\hat{\theta}\cos^2\hat{\theta})\,, \tag{C2}$$

where $\hat{\theta}$ is the phase angle with the symmetry axis, and

$$\sigma \equiv \left(\frac{V_{P0}}{V_{S0}}\right)^2 (\epsilon - \delta)\,. \tag{C3}$$

Our first goal is to express the group velocity and group angle for both P- and S-waves (Figure 2) through the slowness p_{int}. Let us denote the angle between the phase-velocity (slowness) vector of the downgoing P-wave and the reflector normal (pointing upward) by $\bar{\theta}_P$ (Figure C1). Then the phase angle $\hat{\theta}$ with the symmetry axis is equal to $\bar{\theta}_P - \phi$, and equation (C1) can be written as

$$V_P(\bar{\theta}_P) = V_{P0}\,[1 + \delta \sin^2(\bar{\theta}_P - \phi) + (\epsilon - \delta)\sin^4(\bar{\theta}_P - \phi)]\,. \tag{C4}$$

In the linearized weak-anisotropy approximation, group velocity (at the group angle) is equal to phase velocity. Also, we can use the isotropic relationship between the phase angle $\bar{\theta}_P$ and p_{int} because $\bar{\theta}_P$ is contained only in terms already linear in the anisotropic parameters. Hence, the group velocity of the P-wave is given by

$$g_P(p_{\text{int}}) = V_{P0}\,[1 + \delta \sin^2(\bar{\theta}_{\text{is},P} - \phi) + (\epsilon - \delta)\sin^4(\bar{\theta}_{\text{is},P} - \phi)]\,, \tag{C5}$$

where

$$\sin\bar{\theta}_{\mathrm{is},P} = p_{\mathrm{int}}\, V_{P0}\,; \qquad \cos\bar{\theta}_{\mathrm{is},P} = -\sqrt{1-(p_{\mathrm{int}}\, V_{P0})^2}\,. \tag{C6}$$

Next, we need to find the P-wave group angle θ_P^{gr} [equation (A1)] as a function of p_{int}. For the phase angle $\bar{\theta}_P$ we have

$$\sin\bar{\theta}_P = p_{\mathrm{int}}\, V_P = p_{\mathrm{int}}\, V_{P0}\,(1+\alpha_{\mathrm{anis},P}) \tag{C7}$$

and

$$\cos\bar{\theta}_P = -\sqrt{1-(p_{\mathrm{int}}\, V_{P0})^2}\left[1 - \frac{(p_{\mathrm{int}}\, V_{P0})^2}{1-(p_{\mathrm{int}}\, V_{P0})^2}\,\alpha_{\mathrm{anis},P}\right], \tag{C8}$$

where

$$\alpha_{\mathrm{anis},P} \equiv \delta\sin^2(\bar{\theta}_{\mathrm{is},P}-\phi) + (\epsilon-\delta)\sin^4(\bar{\theta}_{\mathrm{is},P}-\phi)\,. \tag{C9}$$

Using the weak-anisotropy relationship between the group and phase angles in TI media (Thomsen, 1986) and taking into account that the P-wave propagates upward from the reflection point yields

$$\tan\theta_P^{\mathrm{gr}} = -\tan(\bar{\theta}_P-\phi)\,[1+2\delta+4(\epsilon-\delta)\sin^2(\bar{\theta}_{\mathrm{is},P}-\phi)]\,. \tag{C10}$$

Thus, the weak-anisotropy approximation makes it possible to find explicit expressions for group velocity and group angle in terms of the slowness projection p_{int}. Substituting $\sin\bar{\theta}_P$ and $\cos\bar{\theta}_P$ from equations (C7) and (C8) into equation (C10) and further linearizing in the anisotropic parameters, we obtain

$$\tan\theta_P^{\mathrm{gr}} = -\tan(\bar{\theta}_{\mathrm{is},P}-\phi)\left[1+2\delta+4(\epsilon-\delta)\sin^2(\bar{\theta}_{\mathrm{is},P}-\phi) + \alpha_{\mathrm{anis},P}\,\frac{\tan\bar{\theta}_{\mathrm{is},P}}{\sin(\bar{\theta}_{\mathrm{is},P}-\phi)\cos(\bar{\theta}_{\mathrm{is},P}-\phi)}\right]. \tag{C11}$$

From equation (C10) it also follows that

$$\frac{1}{\cos\theta_P^{\mathrm{gr}}} = -\frac{1}{\cos(\bar{\theta}_P-\phi)}\,\{1+\sin^2(\bar{\theta}_{\mathrm{is},P}-\phi)\,[2\delta+4(\epsilon-\delta)\sin^2(\bar{\theta}_{\mathrm{is},P}-\phi)]\}\,. \tag{C12}$$

Combining equations (C5) and (C12) gives the term $(1/g_P\cos\theta_P^{\mathrm{gr}})$ needed to find the traveltime along the P-wave leg:

$$\frac{1}{g_P\cos\theta_P^{\mathrm{gr}}} = -\frac{1}{V_{P0}\,\cos(\bar{\theta}_{\mathrm{is},P}-\phi)}\left[1+2(\epsilon-\delta)\sin^4(\bar{\theta}_{\mathrm{is}}-\phi) + \alpha_{\mathrm{anis,P}}\,\frac{\cos\phi}{\cos\bar{\theta}_{\mathrm{is,P}}\,\cos(\bar{\theta}_{\mathrm{is},P}-\phi)}\right]. \tag{C13}$$

Similar algebraic transformations yield the corresponding expressions for the S-wave leg:

$$\tan\theta_S^{\mathrm{gr}} = \tan(\bar{\theta}_{\mathrm{is},S}-\phi)\left[1+2\sigma-4\sigma\sin^2(\bar{\theta}_{\mathrm{is},S}-\phi) + \alpha_{\mathrm{anis},S}\,\frac{\tan\bar{\theta}_{\mathrm{is},S}}{\sin(\bar{\theta}_{\mathrm{is},S}-\phi)\cos(\bar{\theta}_{\mathrm{is},S}-\phi)}\right], \tag{C14}$$

$$\frac{1}{g_S\cos\theta_S^{\mathrm{gr}}} = \frac{1}{V_{S0}\cos(\bar{\theta}_{\mathrm{is},S}-\phi)}\left[1-2\sigma\sin^4(\bar{\theta}_{\mathrm{is},S}-\phi) + \alpha_{\mathrm{anis},S}\,\frac{\cos\phi}{\cos\bar{\theta}_{\mathrm{is},S}\,\cos(\bar{\theta}_{\mathrm{is},S}-\phi)}\right], \tag{C15}$$

where

$$\alpha_{\mathrm{anis},S} \equiv \sigma\sin^2(\bar{\theta}_{\mathrm{is},S}-\phi)\cos^2(\bar{\theta}_{\mathrm{is},S}-\phi) \tag{C16}$$

and

$$\sin\bar{\theta}_{\mathrm{is},S} = p_{\mathrm{int}}\, V_{S0}\,; \qquad \cos\bar{\theta}_{\mathrm{is},S} = \sqrt{1-(p_{\mathrm{int}}\, V_{S0})^2}\,. \tag{C17}$$

Note that the terms involving anisotropic coefficients in equations (C14) and (C15) can be obtained from the anisotropic terms in the corresponding P-wave equations (C11) and (C13) by making the following substitutions: V_{P0} should be replaced with V_{S0}, δ – with σ, and ϵ set to zero. Equations (C11), (C13), (C14), and (C15) are sufficient for obtaining the traveltime and offset for the P-wave leg using the general relationships (A4)–(A8).

Prior to obtaining the attributes associated with the traveltime minimum, it is necessary to determine the corresponding slowness projection $p_{\mathrm{int}}^{\mathrm{min}}$. To derive concise approximations for NMO velocity and other moveout attributes, hereafter we drop all terms with the cubic and higher powers of $\sin\phi$ (i.e., the dip is assumed to be relatively mild). Linearizing equation (B17) in the anisotropic parameters and keeping terms up to quadratic in $\sin\phi$ yields

$$p_{\text{int}}^{\min} = \frac{\sin\phi}{2}\left(\frac{1}{V_{S0}} - \frac{1}{V_{P0}}\right). \tag{C18}$$

Equation (C18) is fully equivalent to the isotropic result (B20), which can be shown by recalculating $p_{\text{int}}^{\min}$ into the corresponding horizontal slowness $p_P(p_{\text{int}}^{\min})$.

Next, we substitute $p_{\text{int}}^{\min}$ from equation (C18) into equations (C11), (C13), (C14), and (C15), carry out expansion in $\sin\phi$ and truncate the series after the $\sin^2\phi$-term. The results allows us to obtain the minimum traveltime $t_{\min}$ and the corresponding offset $x_{\min}$ from the general equations (A4)–(A8) using symbolic software Mathematica:

$$t_{\min} = z_{\text{CMP}}\,\frac{(V_{P0}+V_{S0})}{V_{P0}V_{S0}}\left\{1 - \frac{\sin^2\phi\,(V_{P0}+V_{S0})^2}{8\,V_{P0}V_{S0}} + \frac{\sin^2\phi\,(V_{P0}+V_{S0})}{4\,V_{S0}^2}\left[V_{P0}\,(\delta-\epsilon) - V_{S0}\delta\right]\right\}, \tag{C19}$$

$$x_{\min} = z_{\text{CMP}}\,\frac{\sin\phi}{2\,V_{P0}\,V_{S0}^2}\,(V_{P0}+V_{S0})\left[2\,V_{P0}^2(\delta-\epsilon) + V_{P0}V_{S0}\,(1+2\,\delta) - V_{S0}^2\right]. \tag{C20}$$

Next, we introduce the ray parameter (horizontal slowness) p_{P0} of the pure P-wave reflection recorded at zero offset:

$$p_{P0} = \frac{\sin\phi}{V_P(\phi)} \approx \frac{\sin\phi}{V_{P0}}. \tag{C21}$$

Equation (C21) has a purely "isotropic" form because the anisotropic terms in p_{P0} are multiplied with high powers of $\sin\phi$ neglected in our approximation.

Combining equations (C19), (C20), and (C21) and dropping cubic and higher-order terms in p_{P0}, we find

$$\frac{x_{\min}}{t_{\min}} = \frac{p_{P0}\,V_{P0}^2}{2\gamma}\left[(\gamma-1) + 2(\delta\gamma-\sigma)\right], \tag{C22}$$

where $\gamma \equiv V_{P0}/V_{S0}$.

Likewise, the weak-anisotropy, mild-dip approximation for the spatial derivative of the minimum traveltime (C19) is given by

$$\frac{dt_{\min}}{dy_{\text{CMP}}} = \tan\phi\,\frac{dt_{\min}}{dz_{\text{CMP}}} = p_{P0}\,(1+\gamma). \tag{C23}$$

To obtain the weak-anisotropy approximation for normal-moveout velocity, we linearize the exact equation (B14) in the anisotropic parameters. Expanding the linearized version of equation (B14) in $\sin\phi$ up to the quadratic term and substituting $p_{\text{int}}^{\min}$ from equation (C18) leads to the following form of $V_{\text{nmo},PS}$ (this result was also obtained in Mathematica):

$$\begin{aligned} V_{\text{nmo},PS}^{-2} &= \frac{1}{V_{P0}V_{S0}} - \frac{\sin^2\phi}{8\,V_{P0}^3V_{S0}^3}\left[3\,V_{P0}^4 - 2\,V_{P0}^3V_{S0} + 6\,V_{P0}^2V_{S0}^2 - 2\,V_{P0}V_{S0}^3 + 3\,V_{S0}^4\right] \\ &+ \frac{\epsilon}{2\,V_{P0}V_{S0}^4(V_{P0}+V_{S0})}\left[-4\,V_{P0}^2V_{S0}^2 + \sin^2\phi\left(3\,V_{P0}^4 - 11\,V_{P0}^3V_{S0} - V_{P0}^2V_{S0}^2 + 3\,V_{P0}V_{S0}^3 + 6\,V_{S0}^4\right)\right] \\ &+ \frac{\delta\,(V_{S0}-V_{P0})}{2\,V_{P0}^2V_{S0}^4(V_{P0}+V_{S0})}\left[-4\,V_{P0}^2V_{S0}^2 + \sin^2\phi\left(3\,V_{P0}^4 - 8\,V_{P0}^3V_{S0} - 6\,V_{P0}^2V_{S0}^2 - 8\,V_{P0}V_{S0}^3 + 3\,V_{S0}^4\right)\right]. \end{aligned} \tag{C24}$$

Introducing γ and p_{P0}, replacing ϵ with σ, and making further simplifications in equation (C-24) yields the final expression for NMO velocity:

$$\begin{aligned} V_{\text{nmo},PS}^{-2}(p_{P0}) &= V_{\text{nmo},PS}^{-2}(0) - \frac{p_{P0}^2}{8\gamma}\,(3\gamma^4 - 2\gamma^3 + 6\gamma^2 - 2\gamma + 3) \\ &- \frac{p_{P0}^2\,(\gamma-1)}{2\gamma\,(\gamma+1)}\left[6\,\sigma\,(\gamma+1)^2 - (\sigma-\delta)\,\gamma\,(3\gamma^2 - 2\gamma + 3)\right], \end{aligned} \tag{C25}$$

where

$$V_{\text{nmo},PS}^{-2}(0) = \frac{1}{V_{P0}V_{S0}}\left[1 - \frac{2(\sigma+\delta\gamma)}{1+\gamma}\right]. \tag{C26}$$

The approximate slope of the moveout curve at zero offset can be found by linearizing the exact equation (B3) in ϵ and δ. The value of p_{int} corresponding to $x = 0$ satisfies the condition

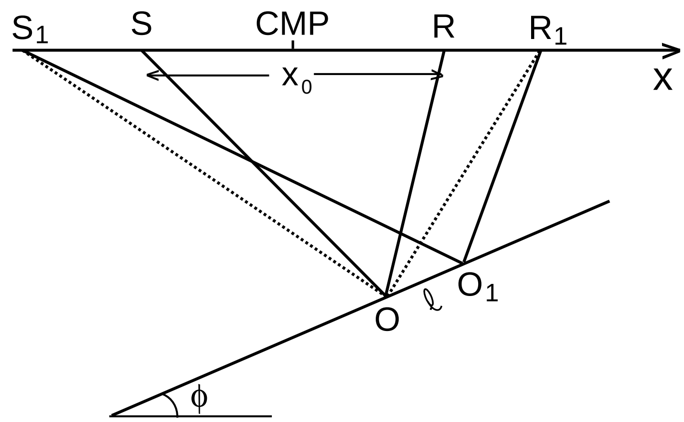

Figure D1. To determine the slope of the moveout curve at the offset $x_0 = SR$, the specular reflection raypath $S_1 O_1 R_1$ in a vicinity of x_0 can be replaced with a non-specular raypath $S_1 O R_1$.

$$q'_P = q'_S \,, \tag{C27}$$

which follows from equation (A17), if we take into account that at $x = 0$ the group-velocity vectors of P- and S-waves are parallel to each other. The mild-dip, weak-anisotropy approximation for the moveout slope at $x = 0$ is given by

$$\left.\frac{dt}{dx}\right|_{x=0} = \frac{p_{P0}}{2\,(1+\gamma)}\,\left[(1-\gamma^2) + 4\gamma\,(\sigma - \delta)\right] . \tag{C28}$$

APPENDIX D: General expression for the slope of reflection moveout

The goal of this appendix is to prove that the apparent slowness (slope) of the CMP moveout curve for any converted or pure reflection is determined by the difference between the ray parameters (slownesses) corresponding to the two legs of the reflected ray. As before, we assume a 2-D model of wave propagation, with the group velocities of the reflected waves confined to the incidence plane. The medium above the reflector, however, is no longer restricted to a single homogeneous layer and may be arbitrary inhomogeneous and anisotropic (with the incidence plane still being a plane of symmetry).

Suppose the reflected wave represents a converted PS mode recorded in CMP geometry (Figure D1). The slope of the moveout curve at any offset x_0 is given by

$$\left.\frac{dt}{dx}\right|_{x_0} = \left.\frac{d(t_P + t_S)}{dx}\right|_{x_0} , \tag{D1}$$

where t_P is the traveltime along segment S_1O_1 and t_S corresponds to O_1R_1 (Figure D1). To relate the moveout slope to the ray parameters of the P- and S-waves, it is convenient to add and subtract from dt/dx the slope of the reflection traveltime $t^{\rm ns}$ along a *non-specular* raypath S_1OR_1. Expressing $t^{\rm ns}$ through the sum of the P and S traveltimes $t_P^{\rm ns}$ and $t_S^{\rm ns}$, we rewrite equation (D1) in the form

$$\left.\frac{dt}{dx}\right|_{x_0} = \left.\frac{d(t_P^{\rm ns} + t_S^{\rm ns})}{dx}\right|_{x_0} + \left.\frac{d(t_P + t_S - t_P^{\rm ns} - t_S^{\rm ns})}{dx}\right|_{x_0} . \tag{D2}$$

Since the P- and S-legs of the non-specular raypath originate from the fixed reflection point O, the slope of the corresponding moveout curve can be expressed as

$$\left.\frac{d(t_P^{\rm ns} + t_S^{\rm ns})}{dx}\right|_{x_0} = \left.\frac{d(t_P^{\rm ns} + t_S^{\rm ns})}{d(2h)}\right|_{h_0} = \frac{1}{2}\left[-p_P(-h_0) + p_S(h_0)\right] , \tag{D3}$$

where $h = x/2$, $h_0 = x_0/2$, p_P and p_S are the horizontal slownesses (ray parameters) evaluated at the surface for the P- and S-rays OS and OR, and the horizontal coordinate axis runs updip.

To prove that the remaining (second) term in the right-hand side of equation (D2) is equal to zero, we consider all possible non-specular reflections with the source-receiver offset $x = S_1R_1$ (Figure D1). The traveltimes of these arrivals can be expanded into a Taylor series in the distance $l = OO_1$ between the specular (O_1) and non-specular reflection point. According to Fermat's principle, the minimum traveltime corresponds to the specular reflection, so the term linear in l in this expansion should vanish. Hence, dropping the cubic and higher-order terms in l, we obtain the following relationship between the nonspecular ($t^{\rm ns} = t_P^{\rm ns} + t_S^{\rm ns}$) and specular ($t = t_P + t_S$) traveltimes:

$$t^{\rm ns} = t + \frac{1}{2} \left. \frac{d^2 t^{\rm ns}}{dl^2} \right|_{l=0} l^2 + \dots . \tag{D4}$$

Therefore, the difference between the traveltimes along the raypaths $S_1 O_1 R_1$ and $S_1 O R_1$ (Figure D1) becomes

$$t - t^{\rm ns} = A(x)\, l^2(x)\,, \tag{D5}$$

where

$$A(x) = -\frac{1}{2} \left. \frac{d^2 t^{\rm ns}}{dl^2} \right|_{l=0} . \tag{D6}$$

Differentiating equation (D5) with respect to x at $x = x_0$ yields

$$\left. \frac{d(t - t^{\rm ns})}{dx} \right|_{x_0} = \left. \frac{dA(x)}{dx}\, l^2(x) \right|_{l=0} + A(x)\, 2l \left. \frac{dl}{dx} \right|_{l=0} = 0\,. \tag{D7}$$

Therefore, the slope of the moveout curve can be determined from the non-specular traveltime [equation (D3)]:

$$\left. \frac{dt}{dx} \right|_{x_0} = \frac{1}{2} \left[-p_P(-h_0) + p_S(h_0) \right] . \tag{D8}$$